Geophysical Research Letters

RESEARCH LETTER
10.1029/2019GL084009

Western Mediterranean Climate Response to Dansgaard/Oeschger Events: New Insights From Speleothem Records

Alexander Budsky[1], Jasper A. Wassenburg[2], Regina Mertz-Kraus[1], Christoph Spötl[3], Klaus Peter Jochum[2], Luis Gibert[4], and Denis Scholz[1]

[1]Institute for Geosciences, Johannes Gutenberg University, Mainz, Germany, [2]Department of Climate Geochemistry, Max Planck Institute for Chemistry, Mainz, Germany, [3]Institute of Geology, Innsbruck University, Innsbruck, Austria, [4]Departament de Mineralogia, Petrologia i Geologia Aplicada, Universitat de Barcelona, Barcelona, Spain

Key Points:
- Western Mediterranean precipitation responded to Greenland interstadials and stadials in a coherent manner
- Dansgaard/Oeschger interstadials were accompanied by humid climate conditions over the western Mediterranean
- Atmospheric circulation patterns did not induce spatial differences in precipitation during the last glacial as they did during the Holocene

Supporting Information:
- Supporting Information S1

Correspondence to:
A. Budsky,
albudsky@students.uni-mainz.de

Citation:
Budsky, A., Wassenburg, J. A., Mertz-Kraus, R., Spötl, C., Jochum, K. P., Gibert, L., & Scholz, D. (2019). Western Mediterranean climate response to Dansgaard/Oeschger events: New insights from speleothem records. *Geophysical Research Letters*, *46*, 9042–9053. https://doi.org/10.1029/2019GL084009

Received 5 JUN 2019
Accepted 22 JUL 2019
Accepted article online 29 JUL 2019
Published online 8 AUG 2019

©2019. The Authors.
This is an open access article under the terms of the Creative Commons Attribution License, which permits use, distribution and reproduction in any medium, provided the original work is properly cited.

Abstract The climate of the western Mediterranean was characterized by a strong precipitation gradient during the Holocene driven by atmospheric circulation patterns. The scarcity of terrestrial paleoclimate archives has precluded exploring this hydroclimate pattern during Marine Isotope Stages 5 to 3. Here we present stable carbon and oxygen isotope records from three flowstones from southeast Iberia, which show that Dansgaard/Oeschger events were associated with more humid conditions. This is in agreement with other records from the Iberian Peninsula, the Mediterranean, and western Europe, which all responded in a similar way to millennial-scale climate variability in Greenland. This general increase in precipitation during Dansgaard/Oeschger events cannot be explained by any present-day or Holocene winter atmospheric circulation pattern. Instead, we suggest that changes in sea surface temperature played a dominant role in determining precipitation amounts in the western Mediterranean.

Plain Language Summary Climate events characterized by a sudden temperature increase of up to 10 °C occurring in less than a few decades during the last glacial are recorded in Greenland ice cores. These abrupt warmings, the Dansgaard/Oeschger events, affected large regions of the Northern Hemisphere. The understanding of the regional response in precipitation during these climate shifts is limited for the western Mediterranean, due to the restricted number of terrestrial climate records that cover the last glacial period at sufficient resolution. Speleothems and their stable isotope compositions allow to trace changes in climate and vegetation based on an accurate chronological framework. Here we present a speleothem stable isotope record that shows that the Dansgaard/Oeschger events were associated with increased rainfall and a denser vegetation in the western Mediterranean. A similar pattern was observed for western Europe and other parts of the Mediterranean, and we propose that this was related to generally higher sea surface temperatures of the surrounding oceans rather than a reorganization of atmospheric circulation.

1. Introduction

During the last glacial period, global climate underwent a series of rapid changes superimposed on a long-term cooling trend (Deplazes et al., 2013; Martrat et al., 2007; North Greenland Ice Core Project members, 2004; Wang et al., 2008). In particular, Greenland ice core records show large, rapid changes in $\delta^{18}O$ values interpreted as changes in temperature (Johnsen et al., 2001; Wolff et al., 2010). This climate variability on millennial timescales with warm Dansgaard/Oeschger (D/O) events—also referred to as Greenland Interstadials (Dansgaard et al., 1993)—and Greenland stadials (Hemming, 2004) is reflected in marine sediment cores from the North Atlantic (Heinrich, 1988; Hemming, 2004; Martrat et al., 2007) as well as the Mediterranean Sea (Cacho et al., 1999; Frigola et al., 2012; Incarbona et al., 2013; Martrat et al., 2004). These millennial-scale fluctuations are assumed to have been linked to the Atlantic Meridional Overturning Circulation (AMOC), which strongly affected climate variability in the Northern Hemisphere during Marine Isotope Stage (MIS) 5b to 3 (96–29 ka; Henry et al., 2016; Li & Born, 2019). The strength of the AMOC controls oceanic heat transport to high northern latitudes (Böhm et al., 2015; Menviel et al., 2014). Concomitantly, the AMOC has a large impact on sea surface temperatures (SST) in the North Atlantic (Pailler & Bard, 2002) as well as the western Mediterranean Sea (Bagniewski et al., 2017; Martrat

et al., 2004). Changes in SST and the position and topography of the ice sheets, in turn, have an impact on the atmospheric circulation (Cacho et al., 2000; Merz et al., 2015; Moreno et al., 2005; Naughton et al., 2009) by influencing the pathways of North Atlantic storm tracks and the position of the Intertropical Convergence Zone (ITCZ; Naughton et al., 2009; Stríkis et al., 2018) and, as a consequence, on effective precipitation in the Mediterranean (Hodge, Richards, Smart, Andreo, et al., 2008; Hodge, Richards, Smart, Ginés, & Mattey, 2008). A decrease or even shutdown of the AMOC is coupled to lower SSTs in the North Atlantic and a southward shifted oceanic thermal front, which results in a more southerly route of the Atlantic jet stream and its associated westerlies (Naughton et al., 2009).

Climate models suggest that on orbital timescales, this mechanism causes an increase in precipitation during cold phases over the western Iberian Peninsula (Hofer, Raible, Merz, et al., 2012; Merz et al., 2015). However, biome data reflect increased dryness, especially during winter (Hofer, Raible, Dehnert, & Kuhlemann, 2012; Wu et al., 2007), which is in agreement with paleoclimate records from SW Europe (Cortina et al., 2016; Denniston et al., 2018; Moreno et al., 2002, 2005). The rapid climate changes during MIS 5b and 3 are also reflected in marine and terrestrial pollen records (Allen et al., 1999; Pons & Reille, 1988; Sánchez Goñi et al., 2008; Tzedakis et al., 2006) and proxy records of precisely dated speleothems (Denniston et al., 2018; Genty et al., 2010).

The present-day climate of the Iberian Peninsula is dominated by several regional atmospheric circulation patterns. For instance, the Western Mediterranean Oscillation (WeMO) and the North Atlantic Oscillation (NAO) lead to strong spatial differences in precipitation (Comas-Bru & McDermott, 2014; Hurrell & Loon, 1997; Martin-Vide & Lopez-Bustins, 2006). Pollen records from offshore sediments provide a wealth of information on last interglacial to glacial vegetation and climate changes, but these data reflect a large region encompassing subregions dominated by different atmospheric circulation patterns. Thus, in order to understand the importance of regional atmospheric circulation patterns, precisely dated terrestrial climate records are needed. However, so far, only very few terrestrial records from the Iberian Peninsula covering MIS 5b to 3 are available. Here we present carbon and oxygen isotope records from three precisely dated flowstones from Cueva Victoria (CV, SE Spain), covering the period from 96 to 45 ka (MIS 5b–3, including D/O events 22 to 12). These records allow to examine how climate variability in the western Mediterranean was related to abrupt climate change in the North Atlantic during the last glacial.

2. Sample Site and Methods

CV (37.63°N, 0.82°W, 40 m above sea level; Figure 1) is located in SE Spain and developed in Triassic limestones and dolostones of the Inner Betic Cordillera (Manteca Martínez & Pina, 2015). The cave system consists of more than 3 km of galleries that were artificially widened by mining activities during the early twentieth century. The climate of the region shows a strong seasonality with warm and dry summers and precipitation maxima in spring and autumn (up to 300 mm/year, mean annual temperature ≈ 17 °C; Figure 1c). This seasonality is also reflected by the monthly $\delta^{18}O$ values of local precipitation, which show an inverse correlation with rainfall and temperature (Araguas-Araguas & Diaz Teijeiro, 2005). On the interannual timescale, the $\delta^{18}O$ values of precipitation do not show a significant correlation to temperature or precipitation (Budsky et al., 2019). Climate is classified as a cold semi-arid climate (BSk) according to the Köppen-Geiger classification (Kottek et al., 2006). The vegetation period lasts from spring to summer and highly depends on rainfall during these seasons (Camarero et al., 2015; Pasho et al., 2011). Precipitation is prevalent during periods characterized by a negative WeMO (Cortesi et al., 2014; Martin-Vide & Lopez-Bustins, 2006; Moreno et al., 2014) index (Figure 1a). The main moisture sources of precipitation are the surrounding Mediterranean and Alboran Sea as well as the North Atlantic (Budsky et al., 2019). There is no direct influence of the NAO (Figure 1b; Hurrell & Loon, 1997) or the ITCZ (Broccoli et al., 2006). Similarly, the main modern European winter circulation patterns, such as the Eastern Atlantic or the Scandinavian pattern (Barnston & Livezey, 1987), have almost no impact on precipitation in SE Spain (Comas-Bru & McDermott, 2014).

Flowstone SR01t (6 cm thick) was sampled from the center of "Sala de las Reuniones", while cores Vic-III-1 and Vic-III-3 were drilled in thick (>50 cm) flowstones in room "Victoria 3" (Ros & Llamusí, 2015). For Vic-III-1 (42 cm) and Vic-III-3 (40.5 cm), we focus on the upper 23 and 8 cm here (supporting information Figure S1), which correspond to the last 96 ka (MIS 5b/c transition). Cave monitoring at CV is not possible

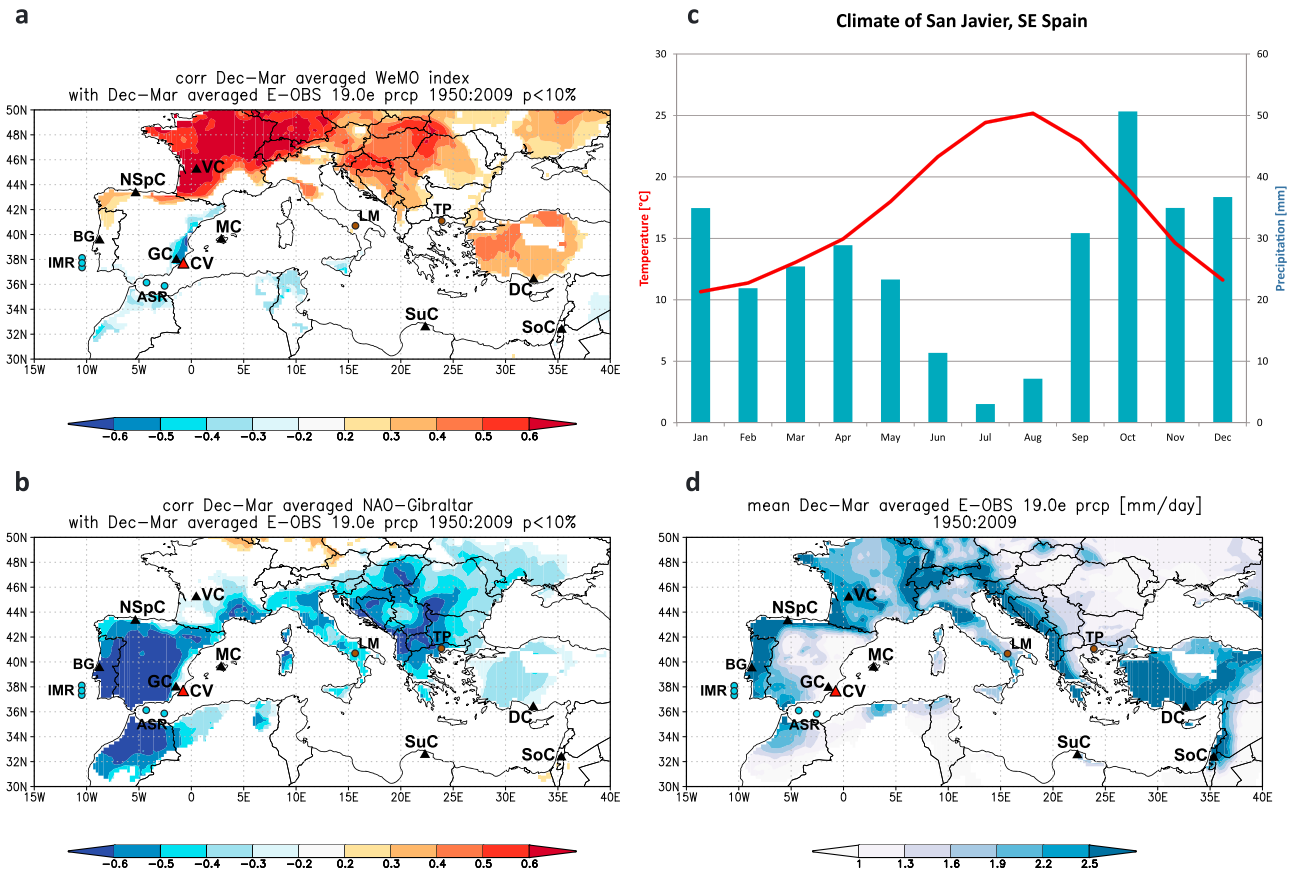

Figure 1. (a) Correlation of observed precipitation (E-OBS 19.0, Cornes et al., 2018) from December to March (1950–2009) with the Western Mediterranean Oscillation (Martin-Vide & Lopez-Bustins, 2006) and (b) the North Atlantic Oscillation index (Jones et al., 1997). (c) Climate diagram for San Javier with temperature (red) and precipitation (blue) displaying strong seasonality. (d) Mean precipitation (1950–2010) for December to March in millimeters per day (Cornes et al., 2018). The correlation (a, b) and precipitation (d) maps were created with the KNMI Climate Explorer (http://climexp.knmi.nl). Speleothem records are indicated by triangles. CV = Cueva Victoria (this study, red triangle); GC = Gitana Cave (Hodge, Richards, Smart, Andreo, et al., 2008); BG = Buraca Gloriosa (Denniston et al., 2018); NSpC = caves in North Spain (Muñoz-García et al., 2007; Stoll et al., 2013); VC = Villars Cave (Genty et al., 2010); MC = Mallorcan Caves (Dumitru et al., 2018; Hodge, Richards, Smart, Ginés, & Mattey, 2008); SuC = Susah Cave (Hoffmann et al., 2016); DC = Dim Cave (Ünal-İmer et al., 2015); SoC = Soreq Cave (Bar-Matthews et al., 2003). Marine sediment cores are indicated by blue circles. ASR = Alboran Sea (ODP161-977, MD95-2043; Martrat et al., 2004; Cacho et al., 1999); IMR = Iberian margin (MD01-2443/4, MD95-2042; Martrat et al., 2007; Daniau et al., 2007; Shackleton et al., 2000). The lake Monticchio (LM; Allen et al., 1999) and Tenaghi Philippon (TP; Tzedakis et al., 2003) records are indicated by brown circles.

due to the lack of active drip sites and the artificial widening of the cave, which strongly altered the natural cave system.

For ^{230}Th/U dating, small pieces (0.05–0.3 g) were cut from the flowstone, prepared by column chemistry (Gibert et al., 2016; Yang et al., 2015), and analyzed using multicollector inductively coupled plasma mass spectrometry at the Max Planck Institute for Chemistry in Mainz (Obert et al., 2016). Samples for stable isotope analysis were milled at an equidistant spacing of 500 μm (Vic-III-1, SR01t) and 250 μm (Vic-III-3), respectively. The obtained powders were analyzed at the University of Innsbruck with a Delta^{plus}XL isotope ratio mass spectrometer linked to a Gasbench II (Spötl, 2011; Spötl & Vennemann, 2003).

3. Results

For all samples used for ^{230}Th/U dating, ^{232}Th was below 10 ng/g. Nevertheless, some samples have a (^{230}Th/^{232}Th) < 200, and detrital contamination may have a significant effect on the ^{230}Th/U-ages (Richards & Dorale, 2003). Thus, ^{230}Th/U ages were corrected for detrital contamination. The (^{232}Th/^{238}U) activity ratio of the detrital material was calculated for each flowstone following the approach of Budsky et al. (2019) by minimizing the total sum of all age inversions. This resulted in a (^{232}Th/^{238}U) activity ratio of 0.24 ± 0.12

for Vic-III-1 and 0.37 ± 0.19 for Vic-III-3, respectively, which are in agreement within uncertainty. For sample SR01t, the correction is negligible due to its low content of detrital material ((^{230}Th/^{232}Th) ≫ 200; Richards & Dorale, 2003). An exception is subsample SR01t-11 ((^{230}Th/^{232}Th) = 49.01). Therefore, we used the mean (^{232}Th/^{238}U) activity ratio of samples Vic-III-1 and Vic-III-3 for detrital correction ((^{232}Th/^{238}U) = 0.31 ± 0.16) for SR01t. The corrected ages range from 95.7 ± 4.7 to 46.2 ± 0.6 ka (Vic-III-1), excluding the uppermost age, which corresponds to the Holocene (Budsky et al., 2019), 92.8 ± 1.8 to 49.9 ± 0.4 ka (Vic-III-3) and 85.4 ± 1.2 to 49.5 ± 1.3 ka (SR01t). The final age models for all flowstones were constructed using the corrected ages and the StalAge algorithm (Scholz & Hoffmann, 2011; Figure S2). Visible hiatuses were included manually into the StalAge age model by fitting the corresponding flowstone sections separately (see supporting information). For very short growth phases consisting of only one ^{230}Th/U-age, we used a mean growth rate of the corresponding longer growth intervals to establish an age-depth model. These short growth intervals were stratigraphically identified by dark layers in thin sections. There is no evidence of dissolution or diagenesis at these growth stops. Thin sections show a pristine elongated/open columnar fabric (cf. Frisia, 2015).

The stable isotope values show a large variability on millennial timescales (Figures 2 and 3). δ^{18}O values range from −6.0‰ to −3.5‰ (Vic-III-1) and −6‰ to −3‰ (Vic-III-3), whereas the δ^{18}O values of SR01t are slightly less negative (−5.5‰ to −3.0‰). The δ^{13}C values of Vic-III-1 and Vic-III-3 range from −11.0‰ to −9.5‰, whereas SR01t shows ~3‰ higher δ^{13}C values. In all samples, the lowest δ^{13}C and δ^{18}O values occur around 85 ka (D/O 21). δ^{18}O and δ^{13}C values correlate positively with r = 0.67 for SR01t, 0.55 for Vic-III-1, and 0.7 for Vic-III-3.

4. Discussion

4.1. Interpretation of the CV Speleothem Record

The three flowstone records from CV cover a long period between the last interglacial and the Last Glacial Maximum, which is only sparsely covered by other paleoclimate archives from SE Spain. The typical D/O pattern as recorded by the North Greenland Ice Core Project ice core (North Greenland Ice Core Project members, 2004; Obrochta et al., 2014; Svensson et al., 2013) is reflected in both the carbon and oxygen isotope records of the CV flowstones with lower values occurring during D/O events and vice versa. This indicates a strong link between climate in the North Atlantic region and SE Spain on millennial timescales. In the overlapping sections, all three flowstones show consistent δ^{13}C and δ^{18}O values (Figures 2 and 3). This replication of the proxy signals confirms that the observed variability is related to climate change above the cave rather than processes within the cave or the karst aquifer. Temporal discrepancies are likely largely due to uncertainties in the chronology of our flowstones, in particular for a few short growth periods that cannot be constrained by more than one ^{230}Th/U-age, and probably to a smaller extent due to the uncertainties of the chronology of North Greenland Ice Core Project (up to 1.5 ka; Svensson et al., 2008; Figure 2).

Budsky et al. (2019) demonstrated a strong influence of effective precipitation on vegetation density and microbiological activity in the soil above CV during the Holocene. Higher δ^{13}C values were interpreted as decreased precipitation during the season of vegetation growth (spring to summer). This interpretation is in agreement with other studies using δ^{13}C values as a proxy for vegetation density (Cerling et al., 1993; Fohlmeister et al., 2011) and soil microbiological activity (Genty et al., 2003; Meyer et al., 2014), which in turn are related to effective precipitation during the growing season (Denniston et al., 2018; Hodge, Richards, Smart, Andreo, et al., 2008; Hodge, Richards, Smart, Ginés, & Mattey, 2008). In addition to these processes occurring in the soil zone, several processes within the aquifer and the cave can result in carbon isotope fractionation, such as prior calcite precipitation, cave ventilation, and the distance of flow on flowstones (Hansen et al., 2017; Johnson et al., 2006; Mühlinghaus et al., 2009; Spötl et al., 2005). Stronger cave ventilation and increased distances of flow lead to enhanced degassing of CO_2 from the solution and precipitation of calcite prior to the sampling site. This may be particularly relevant for sample SR01t, which is associated with the longest distance of flow due to its position in the middle of the cave chamber and may explain the elevated δ^{13}C values compared to the other flowstones. In general, despite their complexity, all processes result in higher δ^{13}C values during drier conditions above the cave. Thus, we interpret higher δ^{13}C values in the CV flowstones as reflecting periods of reduced precipitation/infiltration.

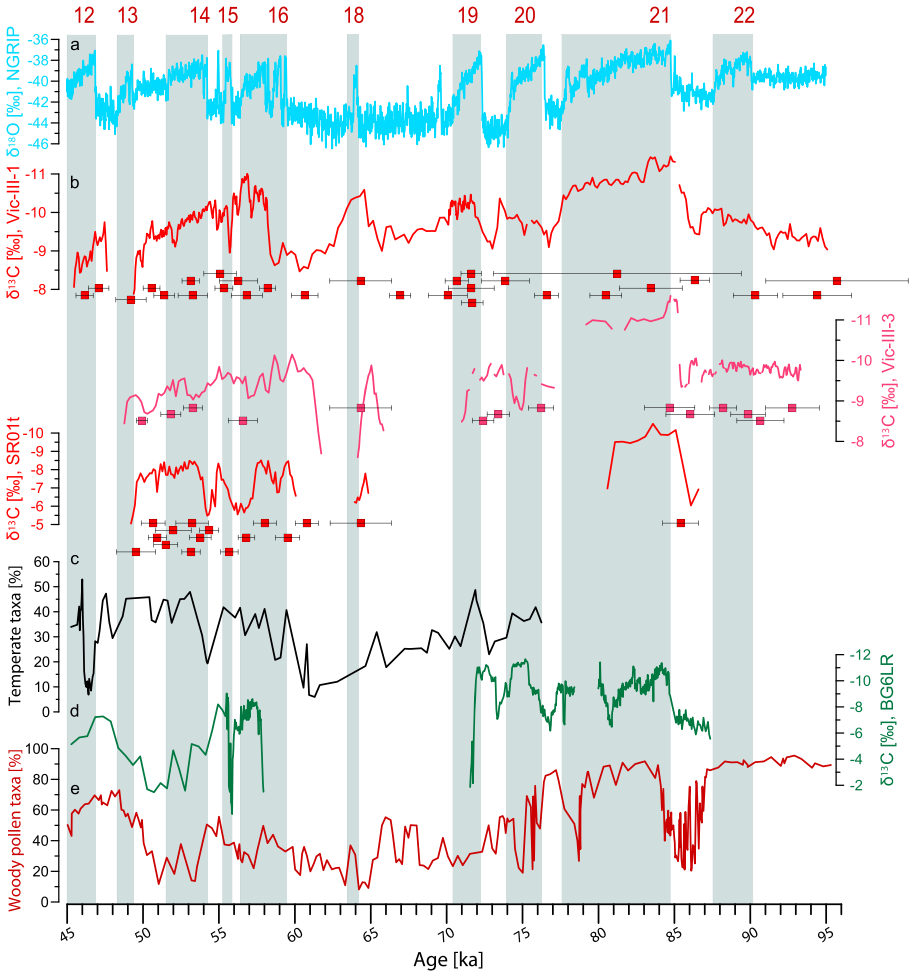

Figure 2. $\delta^{13}C$ values of the three Cueva Victoria flowstones with corresponding $^{230}Th/U$ ages (b), which reflect vegetation density above the cave. Also shown are the NGRIP $\delta^{18}O$ record (a, Obrochta et al., 2014), which shows North Greenland temperature variations, temperate taxa pollen from the Alboran Sea (c, ODP 976, Combourieu Nebout et al., 2002), and the $\delta^{13}C$ values of a speleothem record from Portugal (d, Denniston et al., 2018). In addition, we show the percentage of woody pollen taxa from Lake Monticchio in Italy (e, Allen et al., 1999), which reflect vegetation density. The gray bars indicate the Dansgaard/Oeschger events. NGRIP = North Greenland Ice Core Project.

Lower $\delta^{13}C$ values during D/O events thus suggest increased precipitation in the western Mediterranean during these warm events in the North Atlantic region (Budsky et al., 2019; Genty et al., 2003). This is in agreement with other climate archives from the Mediterranean, such as pollen records from the western Mediterranean (Burjachs et al., 2012; Camuera et al., 2019; Combourieu Nebout et al., 2002; Sánchez Goñi et al., 2008) and Italy (Allen et al., 1999).

The interpretation of $\delta^{18}O$ values in the CV flowstone records is more complex (Budsky et al., 2019). Modern precipitation $\delta^{18}O$ values on a monthly timescale are related to precipitation amount between October and April. Low $\delta^{18}O$ values of monthly precipitation correlate with high rainfall amount and vice versa (Araguas-Araguas & Diaz Teijeiro, 2005). Since summer precipitation with elevated $\delta^{18}O$ values does not infiltrate into the karst rock, the CV flowstones mainly record the more negative $\delta^{18}O$ signal of winter precipitation (Budsky et al., 2019; Carrasco et al., 2006). On the interannual timescale, we thus expect lower $\delta^{18}O$ values for years with increased October–April precipitation, consistent with the interpretation for other Mediterranean speleothem $\delta^{18}O$ records (Ayalon et al., 1998; Ayalon et al., 2002; Bard et al., 2002). However, during D/O events, SSTs on the Iberian margin and in the Alboran Sea were higher (Figure 3) and the continent was warmer (Genty et al., 2010; Martrat et al., 2007), which may have resulted in higher rainfall $\delta^{18}O$

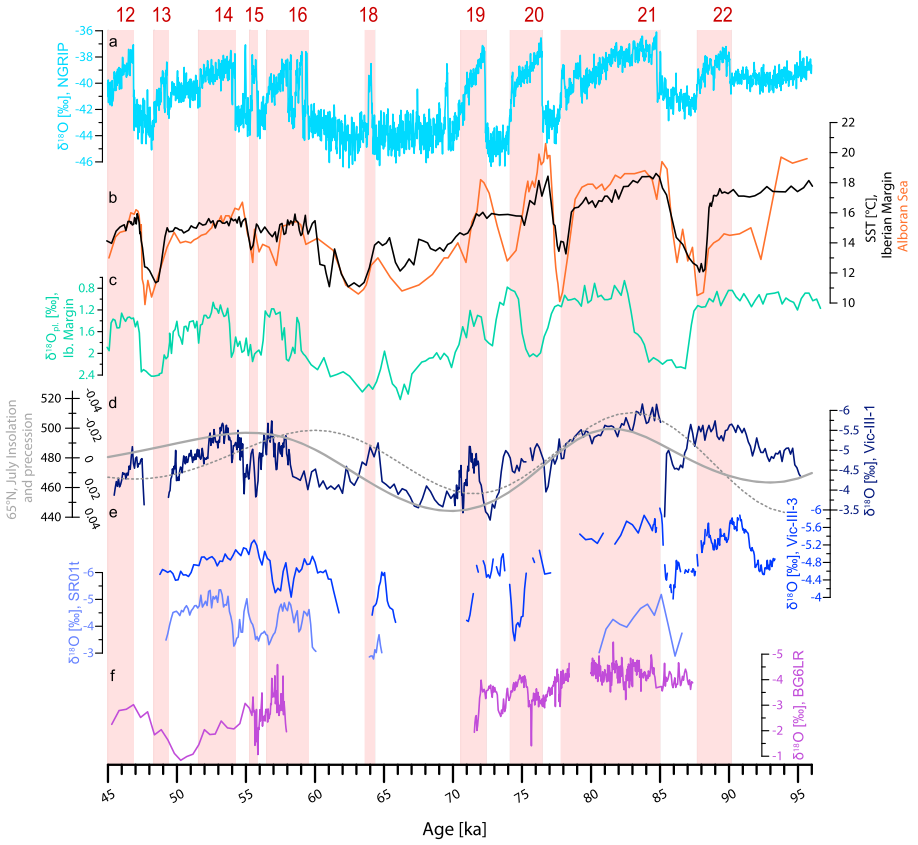

Figure 3. $\delta^{18}O$ values of the three Cueva Victoria flowstones (e) in comparison with NGRIP (a; Obrochta et al., 2014, indicating warm D/O events) as well as SST from the Iberian margin and the Alboran Sea (b; Martrat et al., 2004; Martrat et al., 2007). Also shown are $\delta^{18}O$ values of planktonic foraminifera (*Globigerina bulloides*) from the Iberian margin (c; Vautravers & Shackleton, 2006; Hodell et al., 2013), which reflect changes in both temperature and the $\delta^{18}O$ values of the source for moisture uptake. Long-term changes in flowstone $\delta^{18}O$ values (e) track the 65°N July insolation (d; Laskar et al., 2004) and precession (d, dashed line; Berger, 1978). (f) $\delta^{18}O$ values of a speleothem record from Portugal (Denniston et al., 2018). The reddish bars indicate the D/O events. NGRIP = North Greenland Ice Core Project; D/O = Dansgaard/Oeschger; SST = sea surface temperature.

values (Rozanski et al., 1993) even if Budsky et al. (2019) did not find a significant correlation between temperature and rainfall $\delta^{18}O$ values on interannual timescales. At the same time, warmer cave air results in lower calcite $\delta^{18}O$ values due to the temperature-dependent isotope fractionation between water and calcite (Hansen et al., 2019; Kim & O'Neil, 1997; Tremaine et al., 2011). The interpretation is further complicated because the $\delta^{18}O$ values of precipitation are not directly related to changes in the moisture source (Moreno et al., 2014) preventing the possibility of disentangling precipitation originating in the Atlantic from that originating from the Mediterranean region. This also implies that the transport distance of the water vapor and potential rain-out effects (McDermott, 2004; Mook, 2001) are not dominant because the Mediterranean is the more local moisture source compared to the more distant Atlantic. In addition, temporal changes in the $\delta^{18}O$ value of surface ocean water have to be taken into account, but unfortunately, there is no seawater $\delta^{18}O$ reconstruction available from the region. $\delta^{18}O$ values of planktonic foraminifera in sediment cores from the Iberian margin and the Alboran Sea (Vautravers & Shackleton, 2006), a proxy for both SST and the $\delta^{18}O$ value of seawater, reflect all D/O events (Figure 3b). However, considering the temperature dependence of the $\delta^{18}O$ values of planktonic foraminifera of ~ −0.21‰/°C (Bemis et al., 1998) suggests only minor changes in the $\delta^{18}O$ value of seawater during the D/O events (Figures 3b and 3c). Therefore, we interpret our flowstone $\delta^{18}O$ record as reflecting a combination of the amount of winter precipitation and cave air temperature, with more negative flowstone $\delta^{18}O$ values corresponding to warmer and more humid conditions. This relationship is potentially weakened by the positive relationship between surface air temperature and rainfall $\delta^{18}O$ values.

4.2. Climate Variability on Orbital Timescales

On orbital timescales, the flowstone $\delta^{18}O$ record follows 65°N July insolation, whereby high insolation is associated with low $\delta^{18}O$ and $\delta^{13}C$ values (warm and humid) and vice versa (Figures 3d and 3e; Berger, 1978). Only few terrestrial climate archives in southern Europe and the western Mediterranean cover MIS 5 to 3. For MIS 5c–a, coastal sediments suggest more humid conditions in SE Spain (Mauz et al., 2012). Enhanced precipitation during interglacials is also corroborated by stalagmite growth in northern Iberia (Muñoz-García et al., 2007; Stoll et al., 2013). Located close to CV, the low-resolution Gitana Cave record (Figure 1) is in good agreement with our records on orbital timescales, with higher effective precipitation during interglacials and a cessation of speleothem growth during Heinrich stadial 5 (≈ 46 ka; Hodge, Richards, Smart, Andreo, et al., 2008). This coincides with a prominent sea level drop at circa 45 ka (Siddall et al., 2008) and the termination of calcite deposition in CV. Speleothem $\delta^{13}C$ values from Portugal also suggest that high 65°N summer insolation is associated with higher precipitation (Denniston et al., 2018). In summary, on orbital timescales, precipitation on both the western and the eastern Iberian Peninsula responds to 65°N July insolation.

The 65°N July insolation depends on the interplay between obliquity and precession (Davis & Brewer, 2009). Both lead to a varying latitudinal insolation gradient, which in turn drives the latitudinal temperature gradient and thus climate in higher and lower latitudes by a latitudinal displacement and varying intensity of the midlatitude storm tracks and the tropical Hadley Cell/ITCZ (Schneider et al., 2014; Stríkis et al., 2018). In particular, precession minima are associated with stronger latitudinal shifts of the ITCZ and the midlatitude storm tracks on seasonal timescales and are thus associated with higher seasonality and enhanced autumn/winter precipitation due to higher storm activity in the Mediterranean (Bosmans et al., 2015; Kutzbach et al., 2014; Toucanne et al., 2015). This phenomenon may explain the wetter conditions observed around 80–85 ka in our record, but not those at 50–60 ka (Figure 3). This suggests that the combined signal of 65°N July insolation is more important than precession alone. Higher 65°N July insolation during interglacials is associated with a weaker latitudinal temperature gradient. A higher temperature gradient during glacial periods was associated with a weakened AMOC (Böhm et al., 2015) and leads to stronger and southward shifted westerlies (Merz et al., 2015). Consequently, this should lead to more precipitation on the Iberian Peninsula during glacial periods (Hofer, Raible, Merz, et al., 2012). Interestingly, this is not observed in the western Iberian Peninsula, where glacial periods were characterized by drier conditions, whereas interglacials were relatively wet (Denniston et al., 2018). This apparent controversy may be explained by the fact that the glacials (interglacials) were associated with a reduced (stronger) AMOC and lower (higher) 65°N July insolation, which lead to lower (higher) SSTs. On orbital timescales, SSTs at the Iberian margin are correlated with precipitation at both the western (Denniston et al., 2018) and the eastern Iberian Peninsula (CV; this study). This strongly suggests that SST controlled precipitation on the Iberian Peninsula on orbital timescales, although it remains difficult to assess whether this is related to an increase in winter or summer precipitation or both (Kutzbach et al., 2014).

4.3. Climate Variability on Millennial Timescales

On millennial timescales, we observe that the D/O events are associated with warm and humid conditions, which is even the case for the short-lived D/O events 15 (≈55 ka) and 18 (≈64 ka). In contrast, Greenland stadials are associated with cold and dry conditions at CV (Figure 3). The same pattern is observed across the Iberian Peninsula (Combourieu Nebout et al., 2002; Denniston et al., 2018; Hodge, Richards, Smart, Andreo, et al., 2008; Sánchez Goñi et al., 2008) and in other regions of western Europe (Genty et al., 2003, 2010; Hofer, Raible, Dehnert, & Kuhlemann, 2012; Sánchez Goñi et al., 2013; Wu et al., 2007) and the Mediterranean (Allen et al., 1999; Brauer et al., 2007; Dumitru et al., 2018; Fletcher et al., 2010; Hodge, Richards, Smart, Ginés, & Mattey, 2008).

Warming of the North Atlantic during D/O events is associated with an enhanced AMOC, which results in a decreased temperature gradient. In general, a weakened AMOC during stadials reduces the heat transport to the North concomitant with reduced SSTs (Bagniewski et al., 2017). In combination with the presence of the Laurentide ice sheet, this induces a southward shift of the Hadley Cell, associated with stronger and southward shifted westerlies (Menviel et al., 2014). Stronger and southward shifted westerlies during stadials lead to decreased precipitation over the Iberian Peninsula and vice versa (Bagniewski et al., 2017; Menviel et al., 2014). Nevertheless, from a sediment core off the northwest Iberian coast, a more complex response of

precipitation to Heinrich events 4, 2, and 1 was observed (Naughton et al., 2009). Naughton et al. (2009) suggested that the first phase of the Heinrich events was associated with relatively wet and cold conditions, whereas the second phase was characterized by dry and cold conditions following the displacement of the ocean polar front. However, since the CV record does not cover Heinrich events 4, 2, and 1, this cannot be verified for the eastern Iberian Peninsula. Moreover, the CV record shows drier conditions during stadials and wetter conditions during D/O events.

4.4. Precipitation Patterns: Present-Day Versus Last Glacial Period

The present-day precipitation distribution on the Iberian Peninsula is strongly influenced by several atmospheric circulation patterns including the WeMO and the NAO (Comas-Bru & McDermott, 2014; Cortesi et al., 2014). A negative WeMO index leads to enhanced precipitation in SE Spain, whereas the northern parts remain dry and vice versa (Martin-Vide & Lopez-Bustins, 2006; Figures 1a and 1d). This bipolar precipitation pattern has also been discussed in detail for the Holocene (Budsky et al., 2019). In contrast, the NAO particularly affects precipitation in the regions of the Iberian Peninsula that are not affected by the WeMO (Figure 1b).

During the last glacial D/O events, it is well documented that many regions in addition to southeastern Spain, such as western Europe (Genty et al., 2003; Wainer et al., 2009) and the eastern Mediterranean (Grant et al., 2012; Ünal-İmer et al., 2015), also experienced increased precipitation. This is in agreement with higher tree pollen percentages in Greece (Tenaghi Philippon, Tzedakis et al., 2003) and Italy (Lake Monticchio, Allen et al., 1999) and lower speleothem $\delta^{18}O$ values and growth phases in northern Libya (Hoffmann et al., 2016). Thus, it was more humid during the D/O events in the whole Mediterranean area and western Europe. This simultaneous increase in precipitation associated with the D/O events in this large region cannot be explained by changes in modern winter atmospheric circulation pattern, such as the NAO, the Eastern Atlantic pattern, the Scandinavian pattern, or the WeMO (Comas-Bru & McDermott, 2014; Martin-Vide & Lopez-Bustins, 2006). Instead, we suggest that changes in North Atlantic and Mediterranean SSTs controlled the water vapor content of the atmosphere and regulated changes in precipitation. We emphasize that this general increase in precipitation neither excludes changes in atmospheric circulation during D/O events nor must have been restricted to a specific season.

Such a strong link between SST and precipitation has also been suggested for the last glacial (Denniston et al., 2018; Hodge, Richards, Smart, Ginés, & Mattey, 2008), primarily for the Mediterranean due to instabilities in winter associated with high SSTs during D/O events (Bosmans et al., 2015). In particular, it is well known that the water vapor content of the air over the North Atlantic increased during warmer periods, and these warm and moist air masses were then transported to the western Mediterranean causing an increase in precipitation (Bosmans et al., 2015; Kutzbach & Liu, 1997; Trenberth et al., 1998). During glacials, cool SSTs in the North Atlantic decreased the energy budget over the ocean and the moisture uptake in winter. This resulted in drier conditions in the western Mediterranean (Daniau et al., 2007; Dumitru et al., 2018; Hodge, Richards, Smart, Ginés, & Mattey, 2008; Moreno et al., 2005).

5. Conclusions

Three overlapping flowstone $\delta^{13}C$ and $\delta^{18}O$ records from CV demonstrate that precipitation in SE Spain between MIS 5b and MIS 3 (96–45 ka) was related to North Atlantic climate variability. Warm D/O events were associated with higher precipitation and an expansion of vegetation, even during short D/O events, such as D/O 15 and 18. Cold stadials were associated with lower precipitation and reduced vegetation cover. Warm and humid conditions during D/O events are also recorded by pollen and were associated with an expansion of forests in the Mediterranean region.

Climate of the Iberian Peninsula during the Holocene and the present day shows strong regional differences due to different controlling factors, such as the NAO and the WeMO. However, vast regions in the Mediterranean and western Europe show coherently more humid conditions during D/O events and drier conditions during Greenland stadials. We conclude that this coherent large-scale climate response cannot be explained by present-day winter atmospheric circulation patterns alone. Instead, the SST of the North Atlantic and the Mediterranean Sea played a key role in determining the water vapor content of the atmosphere that controlled precipitation in the western Mediterranean and western Europe.

Acknowledgments

This work was funded by the German Research Foundation (ME3761/2-1 to R. Mertz-Kraus and SCHO 1274/9-1 and SCHO 1274/11-1 to D. Scholz). We thank Andrés Ros and the team of CENM-naturaleza as well as the city of Cartagena for the opportunity to work in Cueva Victoria and the support during field campaigns. The assistance of Beate Schwager in the geochemistry lab of the Max Planck Institute for Chemistry, Mainz, and Manuela Wimmer in the isotope laboratory of the University of Innsbruck is highly appreciated. Marie Froeschmann is thanked for taking isotope samples. The authors gratefully acknowledge the KNMI for providing the online tool "Climate Explorer" (http://climexp.knmi.nl/start.cgi) used in Figure 1 of this publication. Data will be available at the database of the NOAA website. We thank two anonymous reviewers for their thorough and constructive reviews.

References

Allen, J. R. M., Brandt, U., Brauer, A., Hubberten, H. W., Huntley, B., Keller, J., et al. (1999). Rapid environmental changes in southern Europe during the last glacial period. *Nature*, *400*(6746), 740–743. https://doi.org/10.1038/23432

Araguas-Araguas, L. J., & Diaz Teijeiro, M. F. (2005). Isotope composition of precipitation and water vapour in the Iberian Peninsula: First results of the Spanish Network of Isotopes in Precipitation. In *IAEA-TECDOC: Vol. 1453. Isotopic composition of precipitation in the Mediterranean Basin in relation to air circulation patterns and climate: Final report of a coordinated research project, 2000–2004* (pp. 173–190). Vienna: International Atomic Energy Agency.

Ayalon, A., Bar-Matthews, M., & Kaufman, A. (2002). Climatic conditions during marine oxygen isotope stage 6 in the eastern Mediterranean region from the isotopic composition of speleothems of Soreq Cave, Israel. *Geology*, *30*(4), 303–306. https://doi.org/10.1130/0091-7613(2002)030<0303:CCDMOI>2.0.CO;2

Ayalon, A., Bar-Matthews, M., & Sass, E. (1998). Rainfall-recharge relationships within a karstic terrain in the eastern Mediterranean semi-arid region, Israel: $\delta^{18}O$ and δD characteristics. *Journal of Hydrology*, *207*(1-2), 18–31. https://doi.org/10.1016/S0022-1694(98)00119-X

Bagniewski, W., Meissner, K. J., & Menviel, L. (2017). Exploring the oxygen isotope fingerprint of Dansgaard-Oeschger variability and Heinrich events. *Quaternary Science Reviews*, *159*, 1–14. https://doi.org/10.1016/j.quascirev.2017.01.007

Bard, E., Delaygue, G., Rostek, F., Antonioli, F., Silenzi, S., & Schrag, D. P. (2002). Hydrological conditions over the western Mediterranean basin during the deposition of the cold Sapropel 6 (ca. 175 kyr BP). *Earth and Planetary Science Letters*, *202*(2), 481–494. https://doi.org/10.1016/S0012-821X(02)00788-4

Bar-Matthews, M., Ayalon, A., Gilmour, M., Matthews, A., & Hawkesworth, C. J. (2003). Sea–land oxygen isotopic relationships from planktonic foraminifera and speleothems in the eastern Mediterranean region and their implication for paleorainfall during interglacial intervals. *Geochimica et Cosmochimica Acta*, *67*(17), 3181–3199. https://doi.org/10.1016/S0016-7037(02)01031-1

Barnston, A. G., & Livezey, R. E. (1987). Classification, seasonality and persistence of low-frequency atmospheric circulation patterns. *Monthly Weather Review*, *115*(6), 1083–1126. https://doi.org/10.1175/1520-0493(1987)115<1083:CSAPOL>2.0.CO;2

Bemis, B. E., Spero, H. J., Bijma, J., & Lea, D. W. (1998). Reevaluation of the oxygen isotopic composition of planktonic foraminifera: Experimental results and revised paleotemperature equations. *Paleoceanography*, *13*(2), 150–160. https://doi.org/10.1029/98PA00070

Berger, A. L. (1978). Long-term variations of daily insolation and Quaternary climatic changes. *Journal of the Atmospheric Sciences*, *35*(12), 2362–2367. https://doi.org/10.1175/1520-0469(1978)035<2362:LTVODI>2.0.CO;2

Böhm, E., Lippold, J., Gutjahr, M., Frank, M., Blaser, P., Antz, B., et al. (2015). Strong and deep Atlantic Meridional Overturning Circulation during the last glacial cycle. *Nature*, *517*(7532), 73–76. https://doi.org/10.1038/nature14059

Bosmans, J. H. C., Drijfhout, S. S., Tuenter, E., Hilgen, F. J., Lourens, L. J., & Rohling, E. J. (2015). Precession and obliquity forcing of the freshwater budget over the Mediterranean. *Quaternary Science Reviews*, *123*, 16–30. https://doi.org/10.1016/j.quascirev.2015.06.008

Brauer, A., Allen, J. R. M., Mingram, J., Dulski, P., Wulf, S., & Huntley, B. (2007). Evidence for last interglacial chronology and environmental change from southern Europe. *Proceedings of the National Academy of Sciences*, *104*(2), 450–455. https://doi.org/10.1073/pnas.0603321104

Broccoli, A. J., Dahl, K. A., & Stouffer, R. J. (2006). Response of the ITCZ to Northern Hemisphere cooling. *Geophysical Research Letters*, *33*, L01702. https://doi.org/10.1029/2005GL024546

Budsky, A., Scholz, D., Wassenburg, J. A., Mertz-Kraus, R., Spötl, C., Riechelmann, D. F. C., et al. (2019). Speleothem $\delta^{13}C$ record suggests enhanced spring/summer drought in south-eastern Spain between 9.7 and 7.8 ka—A circum-western Mediterranean anomaly? *The Holocene*, *29*(7), 1113–1133. https://doi.org/10.1177/0959683619838021

Burjachs, F., López-García, J. M., Allué, E., Blain, H.-A., Rivals, F., Bennàsar, M., & Expósito, I. (2012). Palaeoecology of Neanderthals during Dansgaard–Oeschger cycles in northeastern Iberia (Abric Romaní): From regional to global scale. *Quaternary International*, *247*, 26–37. https://doi.org/10.1016/j.quaint.2011.01.035

Cacho, I., Grimalt, J. O., Pelejero, C., Canals, M., Sierro, F. J., Flores, J. A., & Shackleton, N. (1999). Dansgaard-Oeschger and Heinrich event imprints in Alboran Sea paleotemperatures. *Paleoceanography*, *14*(6), 698–705. https://doi.org/10.1029/1999PA900044

Cacho, I., Grimalt, J. O., Sierro, F. J., Shackleton, N., & Canals, M. (2000). Evidence for enhanced Mediterranean thermohaline circulation during rapid climatic coolings. *Earth and Planetary Science Letters*, *183*(3-4), 417–429. https://doi.org/10.1016/S0012-821X(00)00296-X

Camarero, J. J., Gazol, A., Tardif, J. C., & Conciatori, F. (2015). Attributing forest responses to global-change drivers: Limited evidence of a CO_2-fertilization effect in Iberian pine growth. *Journal of Biogeography*, *42*(11), 2220–2233. https://doi.org/10.1111/jbi.12590

Camuera, J., Jiménez-Moreno, G., Ramos-Román, M. J., García-Alix, A., Toney, J. L., Anderson, R. S., et al. (2019). Vegetation and climate changes during the last two glacial-interglacial cycles in the western Mediterranean: A new long pollen record from Padul (southern Iberian Peninsula). *Quaternary Science Reviews*, *205*, 86–105. https://doi.org/10.1016/j.quascirev.2018.12.013

Carrasco, F., Andreo, B., Liñán, C., & Mudry, J. (2006). Contribution of stable isotopes to the understanding of the unsaturated zone of a carbonate aquifer (Nerja Cave, southern Spain). *Comptes Rendus Geoscience*, *338*(16), 1203–1212. https://doi.org/10.1016/j.crte.2006.09.009

Cerling, T. E., Wang, Y., & Quade, J. (1993). Expansion of C4 ecosystems as an indicator of global ecological change in the late Miocene. *Nature*, *361*(6410), 344–345. https://doi.org/10.1038/361344a0

Comas-Bru, L., & McDermott, F. (2014). Impacts of the EA and SCA patterns on the European twentieth century NAO-winter climate relationship. *Quarterly Journal of the Royal Meteorological Society*, *140*(679), 354–363. https://doi.org/10.1002/qj.2158

Combourieu Nebout, N., Turon, J. L., Zahn, R., Capotondi, L., Londeix, L., & Pahnke, K. (2002). Enhanced aridity and atmospheric high-pressure stability over the western Mediterranean during the North Atlantic cold events of the past 50 k.y. *Geology*, *30*(10), 863–866. https://doi.org/10.1130/0091-7613(2002)030<0863:EAAAHP>2.0.CO;2

Cornes, R. C., van der Schrier, G., van den Besselaar, E. J. M., & Jones, P. D. (2018). An ensemble version of the E-OBS temperature and precipitation data sets. *Journal of Geophysical Research: Atmospheres*, *123*, 9391–9409. https://doi.org/10.1029/2017JD028200

Cortesi, N., Gonzalez-Hidalgo, J. C., Trigo, R. M., & Ramos, A. M. (2014). Weather types and spatial variability of precipitation in the Iberian Peninsula. *International Journal of Climatology*, *34*(8), 2661–2677. https://doi.org/10.1002/joc.3866

Cortina, A., Grimalt, J. O., Rigual-Hernández, A., Ballegeer, A.-M., Martrat, B., Sierro, F. J., & Flores, J. A. (2016). The impact of ice-sheet dynamics in western Mediterranean environmental conditions during terminations. An approach based on terrestrial long chain n-alkanes deposited in the upper slope of the Gulf of Lions. *Chemical Geology*, *430*, 21–33. https://doi.org/10.1016/j.chemgeo.2016.03.015

Daniau, A.-L., Sánchez-Goñi, M. F., Beaufort, L., Laggoun-Défarge, F., Loutre, M.-F., & Duprat, J. (2007). Dansgaard–Oeschger climatic variability revealed by fire emissions in southwestern Iberia. *Quaternary Science Reviews*, *26*(9-10), 1369–1383. https://doi.org/10.1016/j.quascirev.2007.02.005

Dansgaard, W., Johnsen, S. J., Clausen, H. B., Dahl-Jensen, D., Gundestrup, N. S., Hammer, C. U., et al. (1993). Evidence for general instability of past climate from a 250-kyr ice-core record. *Nature*, *364*(6434), 218–220. https://doi.org/10.1038/364218a0

Davis, B. A. S., & Brewer, S. (2009). Orbital forcing and role of the latitudinal insolation/temperature gradient. *Climate Dynamics*, *32*(2-3), 143–165. https://doi.org/10.1007/s00382-008-0480-9

Denniston, R. F., Houts, A. N., Asmerom, Y., Wanamaker, A. D. Jr., Haws, J. A., Polyak, V. J., et al. (2018). A stalagmite test of North Atlantic SST and Iberian hydroclimate linkages over the last two glacial cycles. *Climate of the Past*, *14*(12), 1893–1913. https://doi.org/10.5194/cp-14-1893-2018

Deplazes, G., Lückge, A., Peterson, L. C., Timmermann, A., Hamann, Y., Hughen, K. A., et al. (2013). Links between tropical rainfall and North Atlantic climate during the last glacial period. *Nature Geoscience*, *6*(3), 213–217. https://doi.org/10.1038/ngeo1712

Dumitru, O. A., Onac, B. P., Polyak, V. J., Wynn, J. G., Asmerom, Y., & Fornós, J. J. (2018). Climate variability in the western Mediterranean between 121 and 67 ka derived from a Mallorcan speleothem record. *Palaeogeography, Palaeoclimatology, Palaeoecology*, *506*, 128–138. https://doi.org/10.1016/j.palaeo.2018.06.028

Fletcher, W. J., Sánchez Goñi, M. F., Allen, J. R. M., Cheddadi, R., Combourieu-Nebout, N., Huntley, B., et al. (2010). Millennial-scale variability during the last glacial in vegetation records from Europe. *Quaternary Science Reviews*, *29*(21-22), 2839–2864. https://doi.org/10.1016/j.quascirev.2009.11.015

Fohlmeister, J., Scholz, D., Kromer, B., & Mangini, A. (2011). Modelling carbon isotopes of carbonates in cave drip water. *Geochimica et Cosmochimica Acta*, *75*(18), 5219–5228. https://doi.org/10.1016/j.gca.2011.06.023

Frigola, J., Canals, M., Cacho, I., Moreno, A., Sierro, F. J., Flores, J. A., et al. (2012). A 500 kyr record of global sea-level oscillations in the Gulf of Lion, Mediterranean Sea: New insights into MIS 3 sea-level variability. *Climate of the Past*, *8*(3), 1067–1077. https://doi.org/10.5194/cp-8-1067-2012

Frisia, S. (2015). Microstratigraphic logging of calcite fabrics in speleothems as tool for palaeoclimate studies. *International Journal of Speleology*, *44*(1), 1–16. https://doi.org/10.5038/1827-806X.44.1.1

Genty, D., Blamart, D., Ouahdi, R., Gilmour, M., Baker, A., Jouzel, J., & Van-Exter, S. (2003). Precise dating of Dansgaard–Oeschger climate oscillations in western Europe from stalagmite data. *Nature*, *421*(6925), 833–837. https://doi.org/10.1038/nature01391

Genty, D., Combourieu-Nebout, N., Peyron, O., Blamart, D., Wainer, K., Mansuri, F., et al. (2010). Isotopic characterization of rapid climatic events during OIS3 and OIS4 in Villars Cave stalagmites (SW-France) and correlation with Atlantic and Mediterranean pollen records. *Quaternary Science Reviews*, *29*(19-20), 2799–2820. https://doi.org/10.1016/j.quascirev.2010.06.035

Gibert, L., Scott, G. R., Scholz, D., Budsky, A., Ferràndez, C., Ribot, F., et al. (2016). Chronology for the Cueva Victoria fossil site (SE Spain): Evidence for Early Pleistocene Afro-Iberian dispersals. *Journal of Human Evolution*, *90*, 183–197. https://doi.org/10.1016/j.jhevol.2015.08.002

Grant, K. M., Rohling, E. J., Bar-Matthews, M., Ayalon, A., Medina-Elizalde, M., Ramsey, C. B., et al. (2012). Rapid coupling between ice volume and polar temperature over the past 150,000 years. *Nature*, *491*(7426), 744–747. https://doi.org/10.1038/nature11593

Hansen, M., Scholz, D., Froeschmann, M.-L., Schöne, B. R., & Spötl, C. (2017). Carbon isotope exchange between gaseous CO_2 and thin solution films: Artificial cave experiments and a complete diffusion-reaction model. *Geochimica et Cosmochimica Acta*, *211*, 28–47. https://doi.org/10.1016/j.gca.2017.05.005

Hansen, M., Scholz, D., Schöne, B. R., & Spötl, C. (2019). Simulating speleothem growth in the laboratory: Determination of the stable isotope fractionation ($\delta^{13}C$ and $\delta^{18}O$) between H_2O, DIC and $CaCO_3$. *Chemical Geology*, *509*, 20–44. https://doi.org/10.1016/j.chemgeo.2018.12.012

Heinrich, H. (1988). Origin and consequences of cyclic ice rafting in the Northeast Atlantic Ocean during the past 130,000 years. *Quaternary Research*, *29*(2), 142–152. https://doi.org/10.1016/0033-5894(88)90057-9

Hemming, S. R. (2004). Heinrich events: Massive late Pleistocene detritus layers of the North Atlantic and their global climate imprint. *Reviews of Geophysics*, *42*, RG1005. https://doi.org/10.1029/2003RG000128

Henry, L. G., McManus, J. F., Curry, W. B., Roberts, N. L., Piotrowski, A. M., & Keigwin, L. D. (2016). North Atlantic Ocean circulation and abrupt climate change during the last glaciation. *Science*, *353*(6298), 470–474. https://doi.org/10.1126/science.aaf5529

Hodell, D., Crowhurst, S., Skinner, L., Tzedakis, P. C., Margari, V., Channell, J. E. T., et al. (2013). Response of Iberian margin sediments to orbital and suborbital forcing over the past 420 ka. *Paleoceanography*, *28*, 185–199. https://doi.org/10.1002/palo.20017

Hodge, E. J., Richards, D. A., Smart, P. L., Andreo, B., Hoffmann, D. L., Mattey, D. P., & González-Ramón, A. (2008). Effective precipitation in southern Spain (~266 to 46 ka) based on a speleothem stable carbon isotope record. *Quaternary Research*, *69*(03), 447–457. https://doi.org/10.1016/j.yqres.2008.02.013

Hodge, E. J., Richards, D. A., Smart, P. L., Ginés, A., & Mattey, D. P. (2008). Sub-millennial climate shifts in the western Mediterranean during the last glacial period recorded in a speleothem from Mallorca, Spain. *Journal of Quaternary Science*, *23*(8), 713–718. https://doi.org/10.1002/jqs.1198

Hofer, D., Raible, C. C., Dehnert, A., & Kuhlemann, J. (2012). The impact of different glacial boundary conditions on atmospheric dynamics and precipitation in the North Atlantic region. *Climate of the Past*, *8*(3), 935–949. https://doi.org/10.5194/cp-8-935-2012

Hofer, D., Raible, C. C., Merz, N., Dehnert, A., & Kuhlemann, J. (2012). Simulated winter circulation types in the North Atlantic and European region for preindustrial and glacial conditions. *Geophysical Research Letters*, *39*, L15805. https://doi.org/10.1029/2012GL052296

Hoffmann, D. L., Rogerson, M., Spötl, C., Luetscher, M., Vance, D., Osborne, A. H., et al. (2016). Timing and causes of North African wet phases during the last glacial period and implications for modern human migration. *Scientific Reports*, *6*(1), 36367. https://doi.org/10.1038/srep36367

Hurrell, J. W., & Loon, H. V. (1997). Decadal variations in climate associated with the North Atlantic Oscillation. *Climatic Change*, *36*(3/4), 301–326. https://doi.org/10.1023/A:1005314315270

Incarbona, A., Sprovieri, M., di Stefano, A., di Stefano, E., Salvagio Manta, D., Pelosi, N., et al. (2013). Productivity modes in the Mediterranean Sea during Dansgaard–Oeschger (20,000–70,000 yr ago) oscillations. *Palaeogeography, Palaeoclimatology, Palaeoecology*, *392*, 128–137. https://doi.org/10.1016/j.palaeo.2013.09.023

Johnsen, S. J., Dahl-Jensen, D., Gundestrup, N., Steffensen, J. P., Clausen, H. B., Miller, H., et al. (2001). Oxygen isotope and palaeotemperature records from six Greenland ice-core stations: Camp Century, Dye-3, GRIP, GISP2, Renland and NorthGRIP. *Journal of Quaternary Science*, *16*(4), 299–307. https://doi.org/10.1002/jqs.622

Johnson, K., Hu, C., Belshaw, N., & Henderson, G. (2006). Seasonal trace-element and stable-isotope variations in a Chinese speleothem: The potential for high-resolution paleomonsoon reconstruction. *Earth and Planetary Science Letters*, *244*(1-2), 394–407. https://doi.org/10.1016/j.epsl.2006.01.064

Jones, P. D., Jonsson, T., & Wheeler, D. (1997). Extension to the North Atlantic Oscillation using early instrumental pressure observations from Gibraltar and south-west Iceland. *International Journal of Climatology*, *17*(13), 1433–1450. https://doi.org/10.1002/(SICI)1097-0088(19971115)17:13<1433::AID-JOC203>3.0.CO;2-P

Kim, S.-T., & O'Neil, J. R. (1997). Equilibrium and nonequilibrium oxygen isotope effects in synthetic carbonates. *Geochimica et Cosmochimica Acta*, *61*(16), 3461–3475. https://doi.org/10.1016/S0016-7037(97)00169-5

Kottek, M., Grieser, J., Beck, C., Rudolf, B., & Rubel, F. (2006). World map of the Köppen-Geiger climate classification updated. *Meteorologische Zeitschrift*, *15*(3), 259–263. https://doi.org/10.1127/0941-2948/2006/0130

Kutzbach, J. E., Chen, G., Cheng, H., Edwards, R. L., & Liu, Z. (2014). Potential role of winter rainfall in explaining increased moisture in the Mediterranean and Middle East during periods of maximum orbitally-forced insolation seasonality. *Climate Dynamics*, *42*(3-4), 1079–1095. https://doi.org/10.1007/s00382-013-1692-1

Kutzbach, J. E., & Liu, Z. (1997). Response of the African monsoon to orbital forcing and ocean feedbacks in the middle Holocene. *Science*, *278*(5337), 440–443. https://doi.org/10.1126/science.278.5337.440

Laskar, J., Robutel, P., Joutel, F., Gastineau, M., Correia, A. C. M., & Levrard, B. (2004). A long-term numerical solution for the insolation quantities of the Earth. *Astronomy and Astrophysics*, *428*(1), 261–285. https://doi.org/10.1051/0004-6361:20041335

Li, C., & Born, A. (2019). Coupled atmosphere-ice-ocean dynamics in Dansgaard-Oeschger events. *Quaternary Science Reviews*, *203*, 1–20. https://doi.org/10.1016/j.quascirev.2018.10.031

Manteca Martínez, J. I., & Pina, R. (2015). Las mineralizaciones ferro-manganesíferas de la mina-cueva Victoria y su contexto geológico. In L. Gibert & C. Ferràndez-Canadell (Eds.), *Geología y Paleontología de Cueva Victoria: Geology and Paleontology of Cueva Victoria Mastia* (Vol. 11–13, pp. 59–74). Cartagena: Revista del Museo Arqueolgico Municipal de Cartagena. Retrieved from http://dialnet.unirioja.es/servlet/articulo?codigo=5093320

Martin-Vide, J., & Lopez-Bustins, J.-A. (2006). The Western Mediterranean Oscillation and rainfall in the Iberian Peninsula. *International Journal of Climatology*, *26*(11), 1455–1475. https://doi.org/10.1002/joc.1388

Martrat, B., Grimalt, J. O., Lopez-Martinez, C., Cacho, I., Sierro, F. J., Flores, J. A., et al. (2004). Abrupt temperature changes in the western Mediterranean over the past 250,000 years. *Science*, *306*(5702), 1762–1765. https://doi.org/10.1126/science.1101706

Martrat, B., Grimalt, J. O., Shackleton, N. J., de Abreu, L., Hutterli, M. A., & Stocker, T. F. (2007). Four climate cycles of recurring deep and surface water destabilizations on the Iberian margin. *Science*, *317*(5837), 502–507. https://doi.org/10.1126/science.1139994

Mauz, B., Fanelli, F., Elmejdoub, N., & Barbieri, R. (2012). Coastal response to climate change: Mediterranean shorelines during the Last Interglacial (MIS 5). *Quaternary Science Reviews*, *54*, 89–98. https://doi.org/10.1016/j.quascirev.2012.02.021

McDermott, F. (2004). Palaeo-climate reconstruction from stable isotope variations in speleothems: A review. *Quaternary Science Reviews*, *23*(7-8), 901–918. https://doi.org/10.1016/j.quascirev.2003.06.021

Menviel, L., Timmermann, A., Friedrich, T., & England, M. H. (2014). Hindcasting the continuum of Dansgaard/Oeschger variability: Mechanisms, patterns and timing. *Climate of the Past*, *10*(1), 63–77. https://doi.org/10.5194/cp-10-63-2014

Merz, N., Raible, C. C., & Woollings, T. (2015). North Atlantic eddy-driven jet in interglacial and glacial winter climates. *Journal of Climate*, *28*(10), 3977–3997. https://doi.org/10.1175/JCLI-D-14-00525.1

Meyer, K. W., Feng, W., Breecker, D. O., Banner, J. L., & Guilfoyle, A. (2014). Interpretation of speleothem calcite $\delta^{13}C$ variations: Evidence from monitoring soil CO_2, drip water, and modern speleothem calcite in central Texas. *Geochimica et Cosmochimica Acta*, *142*, 281–298. https://doi.org/10.1016/j.gca.2014.07.027

Mook, W. G. (Ed) (2001). *Environmental isotopes in the hydrological cycle: Principles and applications. Technical documents in hydrology* (Vol. 39). Paris: UNESCO International Hydrological Programme.

Moreno, A., Cacho, I., Canals, M., Grimalt, J. O., Sánchez-Goñi, M. F., Shackleton, N., & Sierro, F. J. (2005). Links between marine and atmospheric processes oscillating on a millennial time-scale. A multi-proxy study of the last 50,000 yr from the Alboran Sea (western Mediterranean Sea). *Quaternary Land-ocean Correlation Quaternary Land-ocean Correlation*, *24*(14–15), 1623–1636. https://doi.org/10.1016/j.quascirev.2004.06.018

Moreno, A., Cacho, I., Canals, M., Prins, M. A., & Moreno, A. (2002). Saharan dust transport and high-latitude glacial climatic variability: The Alboran Sea record. *Quaternary Research*, *58*(3), 318–328. https://doi.org/10.1006/qres.2002.2383

Moreno, A., Sancho, C., Bartolomé, M., Oliva-Urcia, B., Delgado-Huertas, A., Estrela, M. J., et al. (2014). Climate controls on rainfall isotopes and their effects on cave drip water and speleothem growth: The case of Molinos cave (Teruel, NE Spain). *Climate Dynamics*, *43*(1-2), 221–241. https://doi.org/10.1007/s00382-014-2140-6

Mühlinghaus, C., Scholz, D., & Mangini, A. (2009). Modelling fractionation of stable isotopes in stalagmites. *Geochimica et Cosmochimica Acta*, *73*(24), 7275–7289. https://doi.org/10.1016/j.gca.2009.09.010

Muñoz-García, M. B., Martín-Chivelet, J., Rossi, C., Ford, D. C., & Schwarcz, H. P. (2007). Chronology of Termination II and the Last Interglacial Period in north Spain based on stable isotope records of stalagmites from Cueva del Cobre (Palencia). *Journal of Iberian Geology*, *33*(1), 17–30.

Naughton, F., Sánchez Goñi, M. F., Kageyama, M., Bard, E., Duprat, J., Cortijo, E., et al. (2009). Wet to dry climatic trend in north-western Iberia within Heinrich events. *Earth and Planetary Science Letters*, *284*(3-4), 329–342. https://doi.org/10.1016/j.epsl.2009.05.001

North Greenland Ice Core Project members (2004). High-resolution record of Northern Hemisphere climate extending into the last interglacial period. *Nature*, *431*(7005), 147–151. https://doi.org/10.1038/nature02805

Obert, J. C., Scholz, D., Felis, T., Brocas, W. M., Jochum, K. P., & Andreae, M. O. (2016). ^{230}Th/U dating of Last Interglacial brain corals from Bonaire (southern Caribbean) using bulk and theca wall material. *Geochimica et Cosmochimica Acta*, *178*, 20–40. https://doi.org/10.1016/j.gca.2016.01.011

Obrochta, S. P., Yokoyama, Y., Morén, J., & Crowley, T. J. (2014). Conversion of GISP2-based sediment core age models to the GICC05 extended chronology. *Quaternary Geochronology*, *20*, 1–7. https://doi.org/10.1016/j.quageo.2013.09.001

Pailler, D., & Bard, E. (2002). High frequency palaeoceanographic changes during the past 140 000 yr recorded by the organic matter in sediments of the Iberian margin. *Palaeogeography, Palaeoclimatology, Palaeoecology*, *181*(4), 431–452. https://doi.org/10.1016/S0031-0182(01)00444-8

Pasho, E., Camarero, J. J., de Luis, M., & Vicente-Serrano, S. M. (2011). Impacts of drought at different time scales on forest growth across a wide climatic gradient in north-eastern Spain. *Agricultural and Forest Meteorology*, *151*(12), 1800–1811. https://doi.org/10.1016/j.agrformet.2011.07.018

Pons, A., & Reille, M. (1988). The Holocene- and upper Pleistocene pollen record from Padul (Granada, Spain): A new study. *Palaeogeography, Palaeoclimatology, Palaeoecology*, *66*(3-4), 243–263. https://doi.org/10.1016/0031-0182(88)90202-7

Richards, D. A., & Dorale, J. A. (2003). Uranium-series chronology and environmental applications of speleothems. *Reviews in Mineralogy and Geochemistry*, *52*(1), 407–460. https://doi.org/10.2113/0520407

Ros, A., & Llamusí, J. L. (2015). Reconsrucción y génesis del karst de Cueva Victoria: Reconstruction and genesis of the Cueva Victoria karst. In L. Gibert & C. Ferràndez-Canadell (Eds.), *Geología y Paleontología de Cueva Victoria: Geology and Paleontology of Cueva Victoria Mastia* (Vol. 11–13, pp. 111–125). Cartagena: Revista del Museo Arqueológico Municipal de Cartagena. Retrieved from https://dialnet.unirioja.es/servlet/articulo?codigo=5093425

Rozanski, K., Araguás-Araguás, L., & Gonfiantini, R. (1993). Isotopic patterns in modern global precipitation. In P. K. Swart, K. C. Lohmann, J. McKenzie, & S. Savin (Eds.), *Climate change in continental isotopic records* (pp. 1–36). Washington, DC: American Geophysical Union. https://doi.org/10.1029/GM078p0001

Sánchez Goñi, M. F., Bard, E., Landais, A., Rossignol, L., & D'Errico, F. (2013). Air-sea temperature decoupling in western Europe during the last interglacial-glacial transition. *Nature Geoscience*, *6*(10), 837–841. https://doi.org/10.1038/ngeo1924

Sánchez Goñi, M. F., Landais, A., Fletcher, W. J., Naughton, F., Desprat, S., & Duprat, J. (2008). Contrasting impacts of Dansgaard–Oeschger events over a western European latitudinal transect modulated by orbital parameters. *Quaternary Science Reviews*, *27*(11–12), 1136–1151. https://doi.org/10.1016/j.quascirev.2008.03.003

Schneider, T., Bischoff, T., & Haug, G. H. (2014). Migrations and dynamics of the Intertropical Convergence Zone. *Nature*, *513*(7516), 45–53. https://doi.org/10.1038/nature13636

Scholz, D., & Hoffmann, D. L. (2011). StalAge—An algorithm designed for construction of speleothem age models. *Quaternary Geochronology*, *6*(3-4), 369–382. https://doi.org/10.1016/j.quageo.2011.02.002

Shackleton, N. J., Hall, M. A., & Vincent, E. (2000). Phase relationships between millennial-scale events 64,000–24,000 years ago. *Paleoceanography*, *15*(6), 565–569. https://doi.org/10.1029/2000PA000513

Siddall, M., Rohling, E. J., Thompson, W. G., & Waelbroeck, C. (2008). Marine Isotope Stage 3 sea level fluctuations: Data synthesis and new outlook. *Reviews of Geophysics*, *46*, RG4003. https://doi.org/10.1029/2007RG000226

Spötl, C. (2011). Long-term performance of the Gasbench isotope ratio mass spectrometry system for the stable isotope analysis of carbonate microsamples. *Rapid Communications in Mass Spectrometry*, *25*(11), 1683–1685. https://doi.org/10.1002/rcm.5037

Spötl, C., Fairchild, I. J., & Tooth, A. F. (2005). Cave air control on dripwater geochemistry, Obir Caves (Austria): Implications for speleothem deposition in dynamically ventilated caves. *Geochimica et Cosmochimica Acta*, *69*(10), 2451–2468. https://doi.org/10.1016/j.gca.2004.12.009

Spötl, C., & Vennemann, T. W. (2003). Continuous-flow isotope ratio mass spectrometric analysis of carbonate minerals. *Rapid Communications in Mass Spectrometry*, *17*(9), 1004–1006. https://doi.org/10.1002/rcm.1010

Stoll, H. M., Moreno, A., Mendez-Vicente, A., Gonzalez-Lemos, S., Jimenez-Sanchez, M., Dominguez-Cuesta, M. J., et al. (2013). Paleoclimate and growth rates of speleothems in the northwestern Iberian Peninsula over the last two glacial cycles. *Quaternary Research*, *80*(2), 284–290. https://doi.org/10.1016/j.yqres.2013.05.002

Stríkis, N. M., Cruz, F. W., Barreto, E. A. S., Naughton, F., Vuille, M., Cheng, H., et al. (2018). South American monsoon response to iceberg discharge in the North Atlantic. *Proceedings of the National Academy of Sciences*, *115*(15), 3788–3793. https://doi.org/10.1073/pnas.1717784115

Svensson, A., Andersen, K. K., Bigler, M., Clausen, H. B., Dahl-Jensen, D., Davies, S. M., et al. (2008). A 60 000 year Greenland stratigraphic ice core chronology. *Climate of the Past*, *4*(1), 47–57. https://doi.org/10.5194/cp-4-47-2008

Svensson, A., Bigler, M., Blunier, T., Clausen, H. B., Dahl-Jensen, D., Fischer, H., et al. (2013). Direct linking of Greenland and Antarctic ice cores at the Toba eruption (74 ka BP). *Climate of the Past*, *9*(2), 749–766. https://doi.org/10.5194/cp-9-749-2013

Toucanne, S., Angue Minto'o, C. M., Fontanier, C., Bassetti, M.-A., Jorry, S. J., & Jouet, G. (2015). Tracking rainfall in the northern Mediterranean borderlands during sapropel deposition. *Quaternary Science Reviews*, *129*, 178–195. https://doi.org/10.1016/j.quascirev.2015.10.016

Tremaine, D. M., Froelich, P. N., & Wang, Y. (2011). Speleothem calcite farmed in situ: Modern calibration of $\delta^{18}O$ and $\delta^{13}C$ paleoclimate proxies in a continuously-monitored natural cave system. *Geochimica et Cosmochimica Acta*, *75*(17), 4929–4950. https://doi.org/10.1016/j.gca.2011.06.005

Trenberth, K. E., Branstator, G. W., Karoly, D., Kumar, A., Lau, N.-C., & Ropelewski, C. (1998). Progress during TOGA in understanding and modeling global teleconnections associated with tropical sea surface temperatures. *Journal of Geophysical Research*, *103*(C7), 14,291–14,324. https://doi.org/10.1029/97JC01444

Tzedakis, P. C., Hooghiemstra, H., & Pälike, H. (2006). The last 1.35 million years at Tenaghi Philippon: Revised chronostratigraphy and long-term vegetation trends. *Quaternary Science Reviews*, *25*(23-24), 3416–3430. https://doi.org/10.1016/j.quascirev.2006.09.002

Tzedakis, P. C., McManus, J. F., Hooghiemstra, H., Oppo, D. W., & Wijmstra, T. A. (2003). Comparison of changes in vegetation in northeast Greece with records of climate variability on orbital and suborbital frequencies over the last 450 000 years. *Earth and Planetary Science Letters*, *212*(1-2), 197–212. https://doi.org/10.1016/S0012-821X(03)00233-4

Ünal-İmer, E., Shulmeister, J., Zhao, J.-X., Uysal, I. T., Feng, Y.-X., Nguyen, A. D., & Yüce, G. (2015). An 80 kyr-long continuous speleothem record from Dim Cave, SW Turkey with paleoclimatic implications for the eastern Mediterranean. *Scientific Reports*, *5*(1), 13,560. https://doi.org/10.1038/srep13560

Vautravers, M. J., & Shackleton, N. J. (2006). Centennial-scale surface hydrology off Portugal during Marine Isotope Stage 3: Insights from planktonic foraminiferal fauna variability. *Paleoceanography*, *21*, PA3004. https://doi.org/10.1029/2005PA001144

Wainer, K., Genty, D., Blamart, D., Hoffmann, D., & Couchoud, I. (2009). A new stage 3 millennial climatic variability record from a SW France speleothem. *Palaeogeography, Palaeoclimatology, Palaeoecology*, *271*(1–2), 130–139. https://doi.org/10.1016/j.palaeo.2008.10.009

Wang, Y., Cheng, H., Edwards, R. L., Kong, X., Shao, X., Chen, S., et al. (2008). Millennial- and orbital-scale changes in the East Asian monsoon over the past 224,000 years. *Nature*, *451*(7182), 1090–1093. https://doi.org/10.1038/nature06692

Wolff, E. W., Chappellaz, J., Blunier, T., Rasmussen, S. O., & Svensson, A. (2010). Millennial-scale variability during the last glacial: The ice core record. *Quaternary Science Reviews*, *29*(21-22), 2828–2838. https://doi.org/10.1016/j.quascirev.2009.10.013

Wu, H., Guiot, J., Brewer, S., & Guo, Z. (2007). Climatic changes in Eurasia and Africa at the last glacial maximum and mid-Holocene: Reconstruction from pollen data using inverse vegetation modelling. *Climate Dynamics*, *29*(2-3), 211–229. https://doi.org/10.1007/s00382-007-0231-3

Yang, Q., Scholz, D., Jochum, K. P., Hoffmann, D. L., Stoll, B., Weis, U., et al. (2015). Lead isotope variability in speleothems—A promising new proxy for hydrological change? First results from a stalagmite from western Germany. *Chemical Geology*, *396*, 143–151. https://doi.org/10.1016/j.chemgeo.2014.12.028